Research Paper

PAIN®

OPEN VIDEO

Mrgprd^{Cre} lineage neurons mediate optogenetic allodynia through an emergent polysynaptic circuit

Charles Warwick[a,b], Colleen Cassidy[a,b], Junichi Hachisuka[a,b,c], Margaret C. Wright[a,b], Kyle M. Baumbauer[a,b,d], Peter C. Adelman[a,b], Kuan H. Lee[a,b], Kelly M. Smith[a,b], Tayler D. Sheahan[a,b], Sarah E. Ross[a,b], H. Richard Koerber[a,b,*]

Abstract

Most cutaneous C fibers, including both peptidergic and nonpeptidergic subtypes, are presumed to be nociceptors and respond to noxious input in a graded manner. However, mechanically sensitive, nonpeptidergic C fibers also respond to mechanical input in the innocuous range, so the degree to which they contribute to nociception remains unclear. To address this gap, we investigated the function of nonpeptidergic afferents using the *Mrgprd*^{Cre} allele. In real-time place aversion studies, we found that low-frequency optogenetic activation of *Mrgprd*^{Cre} lineage neurons was not aversive in naive mice but became aversive after spared nerve injury (SNI). To address the underlying mechanisms of this allodynia, we recorded responses from lamina I spinoparabrachial (SPB) neurons using the semi-intact ex vivo preparation. After SNI, innocuous brushing of the skin gave rise to abnormal activity in lamina I SPB neurons, consisting of an increase in the proportion of recorded neurons that responded with excitatory postsynaptic potentials or action potentials. This increase was likely due, at least in part, to an increase in the proportion of lamina I SPB neurons that received input on optogenetic activation of *Mrgprd*^{Cre} lineage neurons. Intriguingly, in SPB neurons, there was a significant increase in the excitatory postsynaptic current latency from *Mrgprd*^{Cre} lineage input after SNI, consistent with the possibility that the greater activation post-SNI could be due to the recruitment of a new polysynaptic circuit. Together, our findings suggest that *Mrgprd*^{Cre} lineage neurons can provide mechanical input to the dorsal horn that is nonnoxious before injury but becomes noxious afterwards because of the engagement of a previously silent polysynaptic circuit in the dorsal horn.

Keywords: Mrgd, SNI, Electrophysiology, Optogenetics, Dorsal horn, Spinoparabrachial, IB4, Pain, Allodynia

1. Introduction

Traditionally, cutaneous C fibers have been categorized into 2 major classes: peptidergic afferents that generally express substance P or calcitonin gene related peptide (CGRP), as well as the so-called nonpeptidergic afferents that express Mrgprd or bind the isolectin B4 (IB4).[3,9] Because both populations respond vigorously to noxious stimuli, it was generally assumed that both types function mainly as nociceptors. Consistent with this idea, ablation studies have suggested that peptidergic afferents are responsible for thermal pain, whereas nonpeptidergic afferents are responsible for mechanical pain.[6] Moreover, because these nociceptive-responsive neurons collectively make up most of C fibers, it was not uncommon to generally equate C-fiber activity with nociception and, by extension, pain.

However, other findings have challenged the presumption that these populations are exclusively pain-inducing nociceptors. In particular, it remains unclear whether the nonpeptidergic subset of IB4-binding afferents signal nociception or whether their function is more nuanced. For instance, although nonpeptidergic, IB4-binding neurons respond to noxious stimuli, they typically show a graded response over a wide range of mechanical forces and, indeed, have the capacity to detect even low-threshold input that is clearly nonnoxious.[23] In support of this idea, human microneurography studies have shown that most mechanically sensitive C fibers are activated by stimulus intensities that are reported as nonpainful.[12,29] Finally, although transient optogenetic activation of Mrgprd neurons in mice was found to cause withdrawal, prolonged exposure was not sufficient to elicit conditioned place aversion.[4] Thus, the degree to which activity in the nonpeptidergic, IB4-binding population is sufficient to drive aversion or pain remains ambiguous.

A second major gap in our understanding is the role of nonpeptidergic afferents in chronic pain. Injuries that give rise to chronic pain, such as spared nerve injury (SNI), cause central changes that alter the way sensory information is integrated by the nervous system.[2,30] One of the most common consequences of these injury-induced changes is allodynia: a phenomenon in

Sponsorships or competing interests that may be relevant to content are disclosed at the end of this article.

[a] Department of Neurobiology, University of Pittsburgh, Pittsburgh, PA, United States, [b] Pittsburgh Center for Pain Research, University of Pittsburgh, Pittsburgh, PA, United States, [c] Spinal Cord Group, Institute of Neuroscience and Psychology, University of Glasgow, Glasgow, United Kingdom, [d] Department of Anatomy and Cell Biology, University of Kansas Medical Center, Kansas City, MO, United States

**Corresponding author. Address: Department of Neurobiology University of Pittsburgh, School of Medicine, 200 Lothrop St., Pittsburgh, PA 15213. Tel.: (412) 648-9518. E-mail address: rkoerber@pitt.edu (H.R. Koerber).*

Supplemental digital content is available for this article. Direct URL citations appear in the printed text and are provided in the HTML and PDF versions of this article on the journal's Web site (www.painjournalonline.com).

PAIN 162 (2021) 2120–2131

http://dx.doi.org/10.1097/j.pain.0000000000002227

which innocuous mechanical stimuli, such as light brushing of the skin, are perceived as noxious. It is generally assumed that the afferents responsible for allodynia are those that are most responsive to innocuous mechanical input, ie, low-threshold mechanoreceptors (LTMRs). However, many nonpeptidergic, IB4-binding neurons frequently respond vigorously to innocuous stimuli, such as brushing, raising the possibility of their involvement in allodynia.[23] Thus, there remains significant uncertainty about both the afferent subtype(s) and the spinal circuits downstream thereof that give rise to allodynia.

Mrgprd^{Cre} lineage neurons mediate optogenetic allodynia through an emergent polysynaptic circuit, which is not aversive in naive mice. However, in the context of SNI-induced neuropathic pain, activation of *Mrgprd*^{Cre} lineage neurons became aversive. We subsequently show that SNI increases the proportion of lamina I spinoparabrachial (SPB) neurons that respond to innocuous brush input and that this increase is likely to be mediated, at least in part, by the activity of *Mrgprd*^{Cre} lineage neurons, which seem to gain access to lamina I SPB neurons by way of an emergent polysynaptic circuit after SNI.

2. Methods

2.1. Animals

The mice used in these experiments were *Mrgprd*$^{tm1.1(cre)An}$,[23] which were obtained from the Mutant Mouse Resource & Research Center at Chapel Hill (Stock No: 036118-UNC); *Trpv1*$^{tm1(cre)Bbm}$,[5] which were obtained from Jax labs (Bar Harbor, ME) (Stock No: 017769); and *Gt(ROSA)26Sor*$^{tm32(CAG-COP4*H134R/EYFP)Hze}$ also known as Ai32 mice,[19] which were obtained from Jax labs (Stock No: 024109). Additional crosses were made to obtain *Mrgprd*^{Cre}; Ai32 and *Trpv1*^{Cre}; Ai32 mice for these experiments. Mice were given free access to food and water and housed under standard laboratory conditions. All experiments were performed using approximately equal number of male and female animals. We did not observe any trends that were suggestive of an effect of sex, so data were pooled; however, we acknowledge that we were not powered to look at sex differences. The use of animals was approved by the Institutional Animal Care and Use Committee of the University of Pittsburgh.

2.2. Ex vivo preparation

The ex vivo somatosensory system preparation has been previously described in detail.[10,20] In brief, adult mice (aged >4 weeks) were anesthetized with a mixture of ketamine and xylazine (90 and 10 mg/kg, respectively) and perfused transcardially with room temperature, oxygenated (95% O_2–5% CO_2) artificial cerebrospinal fluid (aCSF) (in mmol/L: 1.9 KCl, 1.2 KH_2PO_4, 1.3 $MgSO_4$, 2.4 $CaCl_2$, 26.0 $NaHCO_3$, and 10.0 D-glucose) with 253.9 mmol/L sucrose. Spinal cord, L1 to L4 dorsal root ganglia (DRG), saphenous nerve, and innervated skin were dissected free in continuity. After dissection, the preparation was transferred to a separate recording chamber containing oxygenated aCSF in which the sucrose was replaced with 127.0 mmol/L NaCl. The skin was pinned out on a stainless steel grid platform located at the bath–air interface, such that the dermal surface remained perfused with the aCSF while the epidermis was exposed to the air. The platform provided stability during the application of thermal and mechanical stimuli. The bath was then slowly warmed to 31°C before recording.

2.3. Dorsal root ganglia recordings and peripheral stimuli

Intracellular recordings from L3 DRG cells in the chamber were made using quartz microelectrodes (>100 MΩ filled with 1 mol/L potassium acetate). An electric search stimulus was applied at 1.5 Hz through a glass suction electrode applied to the saphenous nerve to locate cells with axons in the saphenous nerve. Cutaneous receptive fields (RFs) were located with a fine paint brush, blunt glass probe, and von Frey hairs. When cells were driven by the nerve but had no mechanical RF, a thermal search was performed by gently applying hot (52°C) and cold (0°C) saline to the surface of skin using a syringe with a 20-gauge needle. If a thermal RF was located, the absence of mechanical sensitivity was confirmed by searching the identified RF using a glass probe. In most cases, the response characteristics of the DRG cell were then determined by applying computer-controlled mechanical and thermal stimuli. The mechanical stimulator consisted of a constant-force controller (Aurora Scientific, Aurora, ON, Canada) attached to a 1-mm diameter plastic disk. Computer-controlled 5-second square waves of 5, 10, 25, 50, and 100 mN were applied to the RF of the cell. After the functional characterization, responsiveness to laser stimulation was determined using an 80-mW, 473-nm wavelength laser and a 200-μm fiber optic cable affixed to a micromanipulator (Laserglow Technologies, Toronto, ON, Canada). The opening of the fiber optic cable was positioned approximately 5 mm from the skin surface.

2.4. Parabrachial injections

Four- to 6-week-old mice were anesthetized with isoflurane and placed in a stereotaxic apparatus. An incision was made to expose the bone, and a small hole was made in the skull with a dental drill. A glass pipette was used to inject 100 nL of FAST DiI oil (2.5 mg/mL; Invitrogen, Carlsbad, CA) into the left lateral parabrachial area at the following coordinates: from lambda, 1.3 mm lateral; from lambdoid suture, 0.5 mm posterior; and from surface, −2.4 mm. The incision was closed with sutures, and the mice were allowed to recover and returned to their home cages. These injections were made at least 5 days before electrophysiological recordings.

2.5. Whole-cell spinal neuron recordings

Neurons were visualized using a fixed-stage upright Olympus microscope equipped with a 40x water immersion objective, a CCD camera (ORCA-ER; Hamamatsu Photonics, Hamamatsu City, Japan), and a monitor. A narrow-beam infrared light-emitting diode (LED) (L850D-06; Marubeni, Tokyo, Japan, emission peak, 850 nm) was positioned outside the bath, as previously described.[10] Projection neurons in lamina I were identified by DiI fluorescence after retrograde labeling in the parabrachial nucleus. Whole-cell patch clamp recordings were made using borosilicate glass microelectrodes pulled using a PC-10 puller (Narishige International, East Meadow, NY). Pipette resistances ranged from 6 to 12 MΩ. Electrodes were filled with a solution containing the following (in mM): 135 potassium gluconate, 5 KCl, 0.5 $CaCl_2$, 5 EGTA, 5 HEPES, and 5 MgATP; pH 7.2. Alexa Fluor 488 (Invitrogen; 25 mM) was added to confirm recording from the targeted cell. Recordings were acquired using an Axopatch 200B amplifier (Molecular Devices, Sunnyvale, CA). The data were low-pass filtered at 2 kHz and digitized at 10 kHz using a Digidata 1322A (Molecular Devices) and stored using Clampex version 10 (Molecular Devices).

2.6. Cutaneous stimulation

The cell's receptive field was determined using a paint brush and 1- to 4-g von Frey filaments. Once the cell's receptive field was located, subsequent stimuli were applied directly to the receptive field for 1 second to determine the cell's response properties. Mini Analysis (Synaptosoft, Decatur, GA) was used for detecting excitatory postsynaptic currents (EPSCs) and action potentials (APs).

2.7. Cell dissociation and pickup for reverse transcription polymerase chain reaction

Dorsal root ganglia–containing labeled cells from *Mrgprd*^{Cre}; Ai32 mice were removed and dissociated as previously described.[1] In brief, DRG were treated with papain (30 U) followed by collagenase CLS2 (10 U) or Dispase type II (7 U), centrifuged (1 minute at 1000 r/minute), triturated in minimal essential medium, plated onto laminin-coated coverslips in 30-mm diameter dishes, and incubated at 37°C for 45 minutes. Dishes were removed and flooded with collection buffer (140 mM NaCl, 10 mM glucose, 10 mM HEPES, 5 mM KCl, 2 mM $CaCl_2$, and 1 mM $MgCl_2$). Single, labeled cells were identified using fluorescence microscopy, picked up using glass capillaries (World Precision Instruments, Sarasota, FL) held by a 4-axis micromanipulator under bright-field optics, and transferred to tubes containing 3 μL of lysis buffer (Epicentre, MessageBOOSTER kit). Cells were collected within 1 hour of removal from the incubator and within 4 hours of removal from the animals.

2.8. Fluorescence in situ hybridization

Mice were anesthetized with isoflurane and rapidly decapitated. The ipsilateral L2 and L3 DRG of mice were removed within 7 minutes, placed into optimal cutting temperature compound (OCT), and flash frozen using 2-methylbutane chilled on dry ice. Tissue was kept on dry ice until cryosectioning. Dorsal root ganglia samples were cryosectioned at 14 μm and mounted directly onto Superfrost Plus slides, and fluorescence in situ hybridization (FISH) studies were performed according to the protocol for fresh frozen samples using the RNAscope Multiplex Fluorescent v1 Assay (Advanced Cell Diagnostics, Newark, CA; 320851) with minor modifications. In brief, DRG sections were fixed for 15 minutes in ice-cold 4% paraformaldehyde and dehydrated with ethanol. Sections were then treated with protease IV for 15 minutes at room temperature. Probes for *enhanced yellow fluorescent protein (eYFP)* (Advanced Cell Diagnostics, eYFP, 312131), *Mrgprd* (Mm-Mrgprd, 417921), *Mrgpra3* (Mm-Mrgpra3, 548161), and *Sst* (Mm-Sst, 404631) were hybridized for 2 hours at 40°C in a humidified oven, and then, a series of incubations was performed to amplify and label target probes with the assigned fluorescence detection channel (C1-C3). Sections were counterstained with DAPI using ProLong Gold Antifade Mountant (Invitrogen, P36931).

2.9. RNAscope imaging and quantification

All DRG sections were imaged and analyzed blinded to both treatment and probe identity. Dorsal root ganglia sections were imaged on an upright epifluorescence microscope (Olympus BX53) at ×20 magnification. Quantification of probes was performed by manual counting of positive cells in 4 to 5 DRG slices per mouse for each combination of probes. A positive cell was defined as a cell with a clearly defined nucleus and fluorescent signal forming a ring around the nucleus. For determining the absolute number of *Mrgprd*^{Cre} neurons in naive or SNI animals, the area of each counted DRG section was calculated using FIJI (ImageJ, NIH), and the number of cells per square area was then calculated for each slice. Once all image acquisition, counting, and analysis were completed, the treatment groups and probe identity were unblinded.

2.10. Single-cell amplification and quantitative polymerase chain reaction

The RNA isolated from each cell was reverse transcribed and amplified using T7 linear amplification (Epicentre, Message BOOSTER kit for cell lysate), run through RNA Clean & Concentrator-5 columns (Zymo Research, Irvine, CA), and analyzed using quantitative polymerase chain reaction, as previously described,[1] using optimized primers and SsoAdvanced SYBR Green Master Mix (Bio-Rad, Hercules, CA). Threshold cycle time (Ct) values were determined for each well.

2.11. Real-time place aversion

Behavioral boxes were constructed from plexiglasses that were 12 (l) × 5 (w) × 10 (h) inches with guides for dividing the boxes into 3 chambers: 2 chambers measuring 5 × 5 inches and 1 measuring 2 × 5 inches in the middle. For optical stimulation, we used blue LED strip light, 120/m, 10 mm wide, by the 5 m reel, 12 VDC, 8.9 W/m, 742 mA/m (centered at 460 nM) and amber LED strip light, 120/m, 10 mm wide, by the 5 m reel, 12 VDC, 8.9 W/m, 742 mA/m (centered at 595 nM) (Environmental Lights, San Diego, CA). Five-inch strips of LEDs were affixed to a 5- × 12-inch metal box (heat sink) covering a 5- × 5-inch area on the ends of the box (one area blue and the other amber), leaving a 2-inch area in the middle free of lights. This box could then be placed under the plexiglass box to illuminate the floor. The LEDs were controlled using a CED 1401 interface. The LEDs were positioned 10 mm below the surface of the plexiglass floor because we found that at this distance, there was no heating of the plexiglass floor over the 15-minute period of observation.

Mice used in the real-time place aversion (RTPA) were first acclimated to the behavioral boxes for 3 days (15 minutes/day) before testing. On the day of testing, the mice were placed in the center compartment and the LEDs turned on and the sliding doors removed, so the mice could move freely throughout the box for 15 minutes. The mice were recorded during this period using a video camera. The videos were then scored offline. All experimenters were blinded to genotype and experimental condition of the mice.

2.12. Spared nerve injury

Mice were anesthetized with isoflurane, and the posterior right hind limb was shaved and cleaned using an aseptic solution. An incision was made over the popliteal fossa and the underlying muscle incised to expose the fossa. The tibial and peroneal nerves were isolated. The 2 nerves were tightly ligated and cut just distal to the ligature. The muscle and skin were sutured and the animals allowed to recover. For sham surgeries, the procedures were the same except for the ligation and transection. Electrophysiological recordings and FISH experiments were performed 1 week after surgery.

2.13. Immunohistochemistry

Deeply anesthetized mice were perfused with 4% paraformaldehyde, and tissue sections of the L3 spinal cord, DRG, and glabrous skin were embedded in OCT and cut on a cryostat at 20 μm. The sections were stained for IB4, CGRP, and eYFP using the following antibodies or probes: anti-GFP (chicken 1:1250; Aves Labs, Tigard, OR), anti-CGRP (rabbit; 1:1000; Chemicon, Temecula, CA), and IB4 (1:250; IB4-conjugated Alexa Fluor 647; Molecular Probes, Eugene, OR). After incubation in primary antiserum for at least 2 hours, tissue was washed and incubated in appropriate fluorescently tagged secondary antibodies (1:500; Jackson Immunoresearch) for 1 hour, followed by Hoecht staining (1:10,000) for 30 minutes. After washing and mounting in Fluoromount (Sigma), sections were viewed and imaged on an Olympus BX53 fluorescence microscope with UPanSApo 10x or 20x objectives.

2.14. Statistical analyses

Data are expressed as the mean ± SEM or as a Superplot[18] that shows both the technical replicates and mean value for each biological replicate. For electrophysiological experiments, dots represent data points from individual neurons combined from all animals. The following tests were used for statistical analyses: Student *t* test for continuous normal data (comparison of 2 groups), χ^2 test or Fisher exact test for categorical data, ordinary 1-way analysis of variance (ANOVA) with Tukey multiple comparisons post hoc test if indicated by the main effect (comparison of >2 groups), 2-way repeated measures ANOVA with Tukey multiple comparisons post hoc test if indicated by the main effect (time course with comparison of 2 or more groups), or a 1-way ANOVA with Šídák multiple comparisons post hoc. All tests were 2 tailed (unless otherwise indicated), and a value of $P < 0.05$ was considered statistically significant in all cases. All statistical analyses were performed using GraphPad Prism 9 software.

3. Results

3.1. Histological and molecular characterization of Mrgprd^{Cre} lineage neurons

To investigate the functional role of IB4-binding neurons, we targeted these neurons genetically using the *Mrgprd*^{Cre} knockin allele that was originally developed by David Anderson.[23] Because Mrgprd shows some developmental expression,[17] we carefully characterized the neurons that are captured by this genetic tool, as assessed using Ai32, a Cre-dependent reporter embedded in the *Rosa* locus that enables expression of a ChR2-eYPF fusion protein.[19] Analysis of cell bodies in lumbar DRG suggested that the *Mrgprd*^{Cre} allele captured approximately 80% of IB4-binding neurons and, similarly, that approximately 80% of IB4-binding neurons expressed ChR2-eYFP (**Figs. 1A–C**). By contrast, most CGRP-expressing DRG neurons did not express ChR2-eYPF (**Figs. 1D and E**). The analysis of the innervation pattern in the lumbar spinal cord showed a similar pattern: *Mrgprd*^{Cre} lineage neurons showed a very high degree of colocalization with IB4 in a band that corresponds approximately to inner lamina II but limited colocalization with CGRP, which primarily targets lamina I and outer lamina II (**Figs. 1F–J**). In the glabrous skin, *Mrgprd*^{Cre}-targeted neurons colocalized with the pan-neuronal marker PGP9.5 and innervated the most superficial aspect of the epidermis (**Figs. 1K–M**).

A number of recent single-cell sequencing studies have suggested that nonpeptidergic afferents can be further subdivided into more refined subtypes characterized by expression of *Mrgprd*, *Mrgpra3*, or *Sst/Nppb*.[22,25,28] To assess whether the *Mrgprd*^{Cre} lineage captures these populations, we performed multiplex FISH of lumbar DRG from *Mrgprd*^{Cre}; Ai32 mice (**Figs. 1N–P**). These experiments revealed that *Mrgprd*-expressing afferents make up 77% of *Eyfp*-labeled neurons, whereas *Mrgpra3*-expressing neurons make up 17% and *Sst*-expressing neurons make up 7% (**Fig. 1Q**). Together, these 3 populations accounted for 99% of Eyfp-labeled cells. Virtually, all *Mrgprd*-expressing neurons expressed Eypf. By contrast, only about half of the *Mrgpra3* and *Sst* populations were recombined with the *Mrgprd*^{Cre} allele. To complement the FISH experiments, we also performed quantitative real-time PCR of individual eYFP-labeled DRG neurons that were freshly dissociated from adult *Mrgprd*^{Cre}; Ai32 mice. These experiments similarly revealed that all genetically marked neurons fell into 1 of 3 apparent cell types: those with high *Mrgprd* (and lacking *Mrgpra3*, *Sst*, *Calca*, and *Tac1*); those with high levels of *Mrgpra3* (as well as *Calca* but little or no *Mrgprd*, *Sst*, and *Tac1*); and those with high levels of *Sst* (and low levels of *Mrgpra3* and *Tac1* but lacking *Mrgprd* and *Calca*). Importantly, this single-cell analysis of eYPF-labeled cells confirmed that *Mrgprd* is no longer detected in the *Mrgpra3* or *Sst* populations in the adult, suggestive of developmental expression (**Fig. 1R**). Thus, the *Mrgprd*^{Cre} lineage faithfully captures most afferents that have traditionally been termed "nonpeptidergic" nociceptors, which include most IB4-binding neurons, but not peptidergic nociceptors, C-LTMRs, or Trpm8-expressing cold or cool detectors. For purposes of comparison, we also visualized the recombination mediated by the *Trpv1*^{Cre} allele. Consistent with previous reports,[5] we observed that *Trpv1*^{Cre} lineage neurons include most cutaneous C fibers, although not C-LTMRs or Trpm8-expressing afferents (shown in Fig. 1S).

3.2. Optogenetic manipulation of Mrgprd^{Cre}

Lineage neurons We next characterized the responses of *Mrgprd*^{Cre} lineage neurons to optogenetic stimulation of the skin with *Mrgprd*^{Cre}; Ai32 mice and the ex vivo preparation, performing intracellular recordings of L3 DRG neurons (**Fig. 2A**). Afferents were categorized as cutaneous C fibers if they responded to electrical stimulation of the saphenous nerve with a conduction velocity of 1.2 m/second or less. Next, the receptive field of a given cutaneous C fiber was identified manually through application of mechanical or thermal stimuli. Thereafter, quantitative phenotyping to natural and optogenetic stimuli was performed using a Peltier thermode, a mechanical stimulator, and a 473-nm laser applied to the skin within the identified receptive field. Typically, *Mrgprd*^{Cre} lineage neurons responded weakly to cooling and vigorously to noxious heat; they also responded to both low-threshold (10 mN) and high-threshold (50 mN) mechanical inputs in a graded manner, consistent with previous characterizations of nonpeptidergic nociceptors.[15,23] Both optogenetic and natural stimulation of the skin elicited APs (**Figs. 2B and C**). We found that a 5-ms pulse of light was sufficient to drive a single action potential, whereas a 300-ms pulse of light was required to observe a doublet. Finally, *Mrgprd*^{Cre} lineage neurons could follow optogenetic stimulation of at least 5 Hz (**Fig. 2C**).

Overall, of 21 cutaneous C fibers that were recorded from *Mrgprd*^{Cre}; Ai32 mice, 15 showed responses to optogenetic stimulation (~70%), consistent with the idea that *Mrgprd*^{Cre} lineage neurons represent most cutaneous C fibers. For comparison, we found that 11 of the 12 (~90%) cutaneous C fibers from *Trpv1*^{Cre}; Ai32 mice could be opto-tagged in this

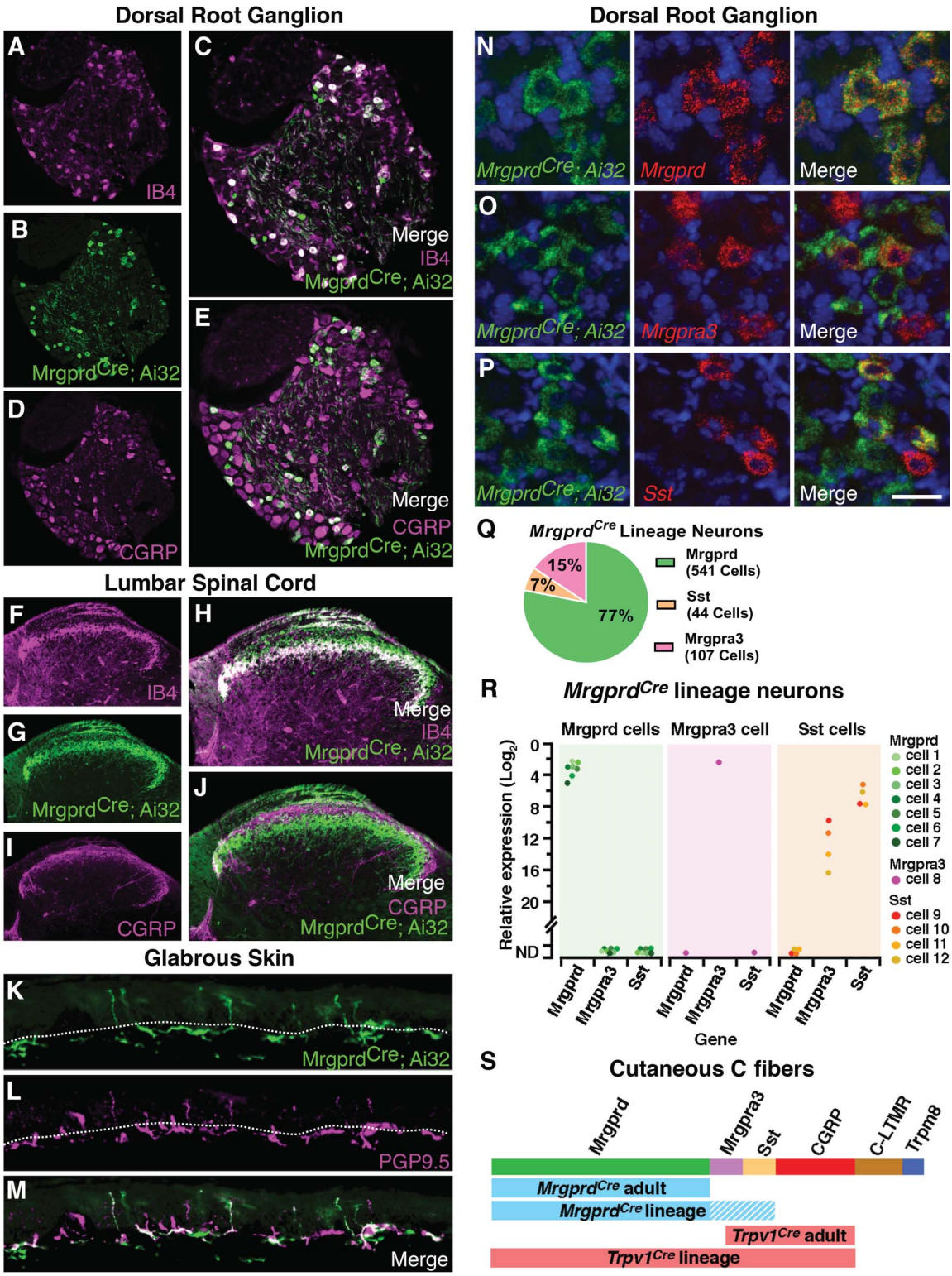

Figure 1. Mrgprd^{Cre} lineage afferents, which comprise Mrgprd, Mrgpra3, and Sst populations, target lamina IIi in the dorsal horn and the superficial aspect of the skin. (A–E) Representative images of a lumbar dorsal root ganglion from a *Mrgprd*^{Cre}; Ai32 mouse that is costained for eYFP and IB4 or CGRP. (F–J) Representative images of the superficial dorsal horn, lumbar level from a *Mrgprd*^{Cre}; Ai32 mouse that is costained for eYFP and IB4 or CGRP. (K–M) Representative images of the glabrous skin from a *Mrgprd*^{Cre}; Ai32 mouse that is costained for eYFP and PGP9.5. Dotted line demarcates the epidermal–dermal junction. (N–P) Representative RNA FISH images of lumbar dorsal root ganglion from a *Mrgprd*^{Cre}; Ai32 mouse that is costained with probes against *Eyfp*, *Mrgprd*, *Mrgpra3*, and *Sst*. (Q) The relative proportion of primary afferent populations captured by the *Mrgprd*^{Cre} lineage as determined by FISH. Data are from 3 mice, with 4 to 5 slices imaged per mouse for a total of 692 *Mrgprd*^{Cre} lineage neurons counted per probe combination. (R) Expression of *Mrgprd*, *Mrgpra3*, *and Sst* mRNA relative to *Gapdh* in individual eYFP-marked *Mrgprd*^{Cre} lineage neurons. Data are presented as the $\log_2$ ΔCT expression relative to *Gapdh* expression within the same cell such that smaller numbers represent higher mRNA expression. Colored dots represent data points from individual cells from a single, representative mouse. (S) Schematic to illustrate the different subtypes of cutaneous C fibers that are captured by the *Mrgprd*^{Cre} and *Trpv1*^{Cre} alleles with developmental (lineage) or adult recombination. FISH, fluorescence in situ hybridization.

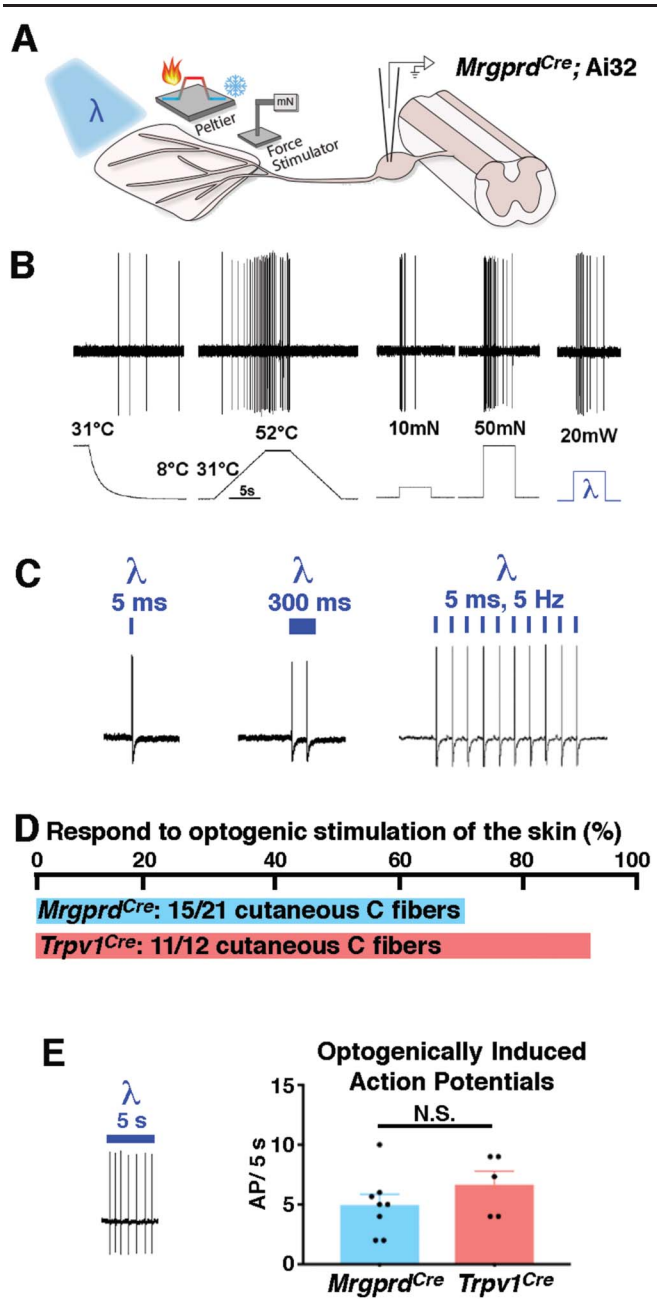

Figure 2. Response of *Mrgprd*^{Cre} lineage afferents to optogenetic stimulation of the skin. (A) Schematic of cutaneous stimulation and intracellular DRG recordings using the ex vivo preparation. (B) Representative responses of *Mrgprd*^{Cre} lineage afferents to cooling, heating, mechanical, and optogenetic stimulation. (C) Representative responses to optogenetic stimulation of *Mrgprd*^{Cre} lineage afferents of varying duration and frequency. (D) Proportion of C fibers that respond to optogenetic stimulation of the skin in *Mrgprd*^{Cre}; Ai32 and *Trpv1*^{Cre}; Ai32 mice, as indicated. (E) Representative recording and quantification of the number of action potentials observed in a given cell on optogenetic stimulation of the skin in *Mrgprd*^{Cre}; Ai32 and *Trpv1*^{Cre}; Ai32 mice, as indicated. Data are mean ± SEM with dots representing data from individual neurons; n = 8 and 5 neurons, respectively, from at least 3 mice. N.S. indicates $P > 0.05$ (unpaired Student *t* test). DRG, dorsal root ganglia.

fashion (**Fig. 2D**), as expected, given the broad recombination mediated by this allele.[5] Importantly, although the *Trpv1*^{Cre} allele captured slightly more C fibers than the *Mrgprd*^{Cre} allele, optogenetic stimulation of individual C fibers from mice of either genotype gave rise to similar numbers of APs, thereby enabling direct comparison of the 2 alleles in behavioral studies (**Fig. 2E**).

3.3. Behavioral responses to optogenetic manipulation of Mrgprd^{Cre} *lineage neurons*

Withdrawal in animals has traditionally been interpreted to represent a pain behavior, but the percept associated with this response is difficult to infer. Previous work has shown that selective optogenetic activation of Mrgprd neurons elicits withdrawal, but not flinching, licking, or guarding.[4] We anticipated that optogenetic stimulation of *Mrgprd*^{Cre} lineage neurons would be at least as aversive, if not more so, because the genetic tool we used captures a larger number of C fibers than that used by Beaudry et al.[4] Although both alleles target the same genetic locus, the degree of recombination using the *Mrgprd*^{Cre} allele is more extensive than the *Mrgprd*^{CreER} allele for 2 reasons: the constitutive *Cre* allele captures more than the adult Mrgprd population due to developmental expression (ie, Sst and Mrgpra3 populations), whereas the *Mrgprd*^{CreER} allele likely captures less than the adult Mrgprd population due to incomplete recombination. Contrary to our expectations, however, we found that the responses of *Mrgprd*^{Cre} mice to optogenetic stimulation of the hind paws appeared quite modest and not qualitatively different than those described for the *Mrgprd*^{CreER} mice.[4] Resting mice generally withdrew their hind paws for a brief moment, as if startled, and then replaced them on the floor, and alert mice rarely responded at all. By sharp contrast, activation of *Trpv1*^{Cre} lineage neurons invariably caused rapid, robust withdrawal that was frequently accompanied by flinching or licking (**Fig. 3A**), just as previously described.[4] These observations raised the possibility that low-frequency optogenetic activation of nonpeptidergic "nociceptors" might not actually be aversive.

Because reflexive behaviors can be hard to interpret and do not readily assess aversion, we turned to nonreflexive behaviors for quantitative analysis. When a stimulus is quite noxious, such as intraplantar formalin, mice will develop conditioned place aversion to the side of the chamber that is associated with the aversive experience. Intriguingly, Beaudry et al. showed that optogenetic activation of *Trpv1*^{Cre} afferents was sufficient for conditioned place aversion, whereas activation of *Mrgprd*^{CreER} afferents was not.[4] However, conditioned place aversion can be difficult to achieve unless the paired stimulus is fairly injurious. We, therefore, developed an RTPA assay to enable the detection of aversive stimuli with higher sensitivity.

Our previous optogenetic characterization had been performed by laser, a coherent light source that is ideal for focal stimulation. However, for the RTPA studies, we were planning to use LEDs, an incoherent light source that is more suitable for widespread activation. To compare the efficacy of optogenetic stimulation by laser and LED, we performed ex vivo skin nerve recordings (**Fig. 3B**). Importantly, stimulation of the skin with either light source gave rise to a similar number of APs in ChR2-expressing *Mrgprd*^{Cre} lineage neurons, indicating that optogenetic stimulation by laser or LED was equally effective at driving activity in ChR2-expressing cells (**Fig. 3C**). With this knowledge, we built a custom RTPA box comprising a stimulation side in which the floor was lined by an array of blue LED lights and a control side in which the floor was lined by an array of amber LED lights, which were separated by a small, unlit middle chamber. These lights were set to run in either the sustained mode, in which the lights were constantly on, or the wind-up mode, in which the lights would flash at 2 Hz for 30 ms per flash. Mice were placed in the RTPA box for 15 minutes, during which time they were allowed to move freely from 1 chamber to another (**Fig. 3D**).

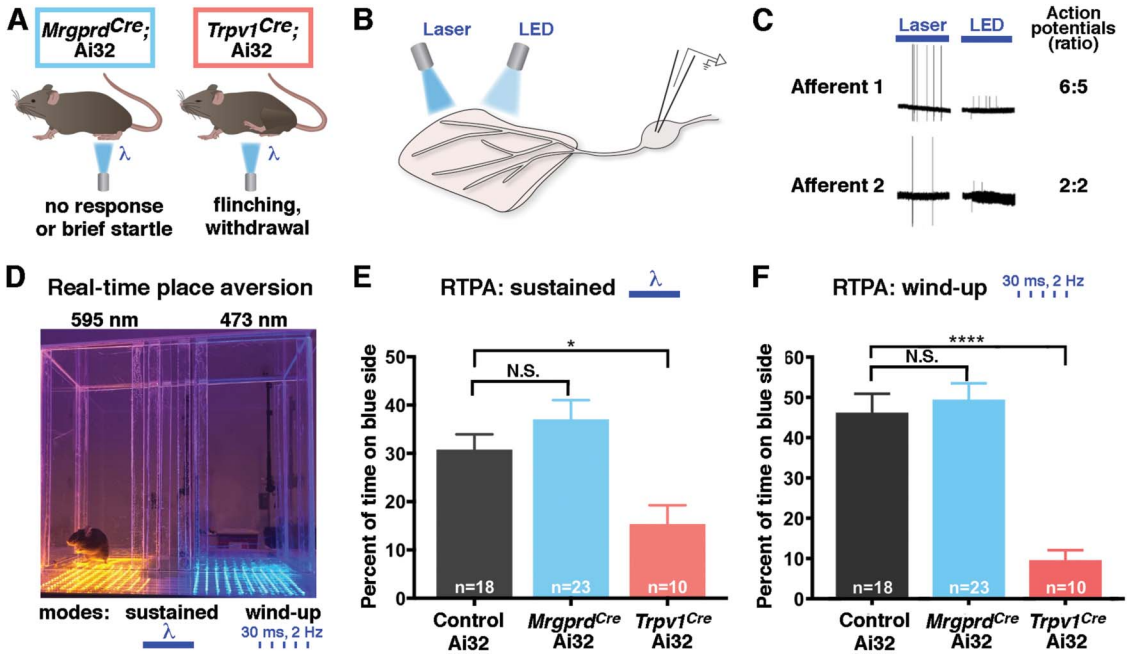

Figure 3. Low-frequency, cutaneous optogenetic activation is aversive in *Trpv1*^{Cre} mice but not *Mrgprd*^{Cre} mice in the naive condition. (A) Schematic illustrating behavioral responses to optogenetic stimulation at the hind paw of *Mrgprd*^{Cre}; Ai32 and *Trpv1*^{Cre}; Ai32 mice. (B) Schematic illustrating comparison of laser- and LED-mediated optogenetic stimulation. (C) Representative traces and quantification of laser-evoked and LED-evoked action potentials in ex vivo recordings from *Mrgprd*^{Cre}; Ai32 mice. (D) Picture of optogenetic real-time place aversion (RTPA) apparatus with amber-light and blue-light sides separated by a middle chamber. (E) In response to sustained light, *Trpv1*^{Cre}; Ai32 mice, but not *Mrgprd*^{Cre}; Ai32 mice, show real-time place aversion to the blue-light side of the apparatus. Data are mean ± SEM; n is number of mice; N.S. indicates $P > 0.05$; *Multiple comparison adjusted P value < 0.05 relative to control Ai32. Significant main effect: $F = 6.793$, $P < 0.0025$ (ordinary 1-way ANOVA with Tukey multiple comparisons post hoc test). (F) In response to flashing light (2 Hz, wind-up mode), *Trpv1*^{Cre}; Ai32 mice, but not *Mrgprd*^{Cre}; Ai32 mice, show real-time place aversion to the blue-light side of the apparatus. Data are mean ± SEM; n is number of mice; N.S. indicates multiple comparison adjusted P value > 0.05; ****Multiple comparison adjusted P value < 0.001 relative to control Ai32. Significant main effect: $F = 18.28$, $P < 0.0001$ (ordinary 1-way ANOVA with Tukey multiple comparisons post hoc test). ANOVA, analysis of variance.

Next, we performed RTPA assays to quantify the aversiveness of optogenetic stimulation. Just as expected, we found that *Trpv1*^{Cre}; Ai32 mice showed significant avoidance of the blue-light side, consistent with the idea that optogenetic activation of nociceptors is unpleasant. By sharp contrast, the time that *Mrgprd*^{Cre}; Ai32 mice spent on the blue-light side was not different than control littermates harboring Ai32 alone (**Fig. 3E**). Similar findings were observed when the LED lights were flashing at 2 Hz to simulate wind-up (**Fig. 3F**). These striking observations suggest that optogenetic activation of *Mrgprd*^{Cre};Ai32 fibers was not aversive, at least not in naive mice.

3.4. Effect of injury: behavioral responses to optogenetic manipulation of Mrgprd^{Cre} *lineage neurons in the context of neuropathic pain*

Although our data suggested that *Mrgprd*^{Cre} lineage neurons can be activated without causing acute pain, a key remaining question was whether they contribute to chronic pain. Allodynia is one of the hallmarks of chronic pain, particularly neuropathic pain.[14] For people who experience allodynia, innocuous everyday experiences, such as fabric moving across the skin, can give rise to shooting pain. Because many nonpeptidergic afferents can respond robustly to dynamic low-threshold stimulation,[23] we hypothesized that *Mrgprd*^{Cre} lineage neurons might contribute to this allodynia. To address this question, we selected to use the SNI model[8] of chronic neuropathic pain (**Fig. 4A**). Although the saphenous nerve remains intact in this model, there is, nevertheless, the potential for the function of afferents to be affected by the injury. We, therefore, measured the responses of *Mrgprd*^{Cre} lineage afferents to optogenetic stimulation of the skin, comparing naive and SNI mice (**Fig. 4B**). Importantly, the number of APs that were elicited was not affected by SNI (**Fig. 4C**). Thus, neuropathic injury did not cause sensitization of *Mrgprd*^{Cre} lineage afferents to optogenetic stimulation.

To address whether SNI altered how the input from *Mrgprd*^{Cre} lineage neurons was integrated in the central nervous system, we performed RTPA assays. Once again, at baseline, the amount of time that naive *Mrgprd*^{Cre}; Ai32 mice spent on the blue-light side was not different than that of control mice, confirming that activity in *Mrgprd*^{Cre} lineage neurons is not aversive in the absence of injury. By contrast, however, optogenetic activation of *Mrgprd*^{Cre} lineage neurons in mice with SNI caused significantly more avoidance than activation of these neurons in naive mice (**Fig. 4D**). Importantly, this optogenetic allodynia was not due to an increase in the number of ChR2-expressing neurons; FISH experiments of L2-L3 revealed that both the total number of afferents that express ChR2 (**Figs. 4E and F**) and the proportion thereof that express *mrgprd*, *Mrgpra3*, and *Sst* (**Figs. 4G and H**) were unchanged after SNI. Taken together, these findings suggest that activity in nonpeptidergic afferents becomes aversive after nerve injury. Moreover, the lack of sensitization postinjury in *Mrgprd*^{Cre} lineage afferents to optogenetic stimulation implied that central mechanisms must mediate optogenetic allodynia due to SNI.

3.5. Modulation of spinoparabrachial neurons by Mrgprd^{Cre} *lineage afferent input*

To investigate the spinal circuitry underlying this phenomenon, we performed whole-cell patch clamp recordings of lamina I

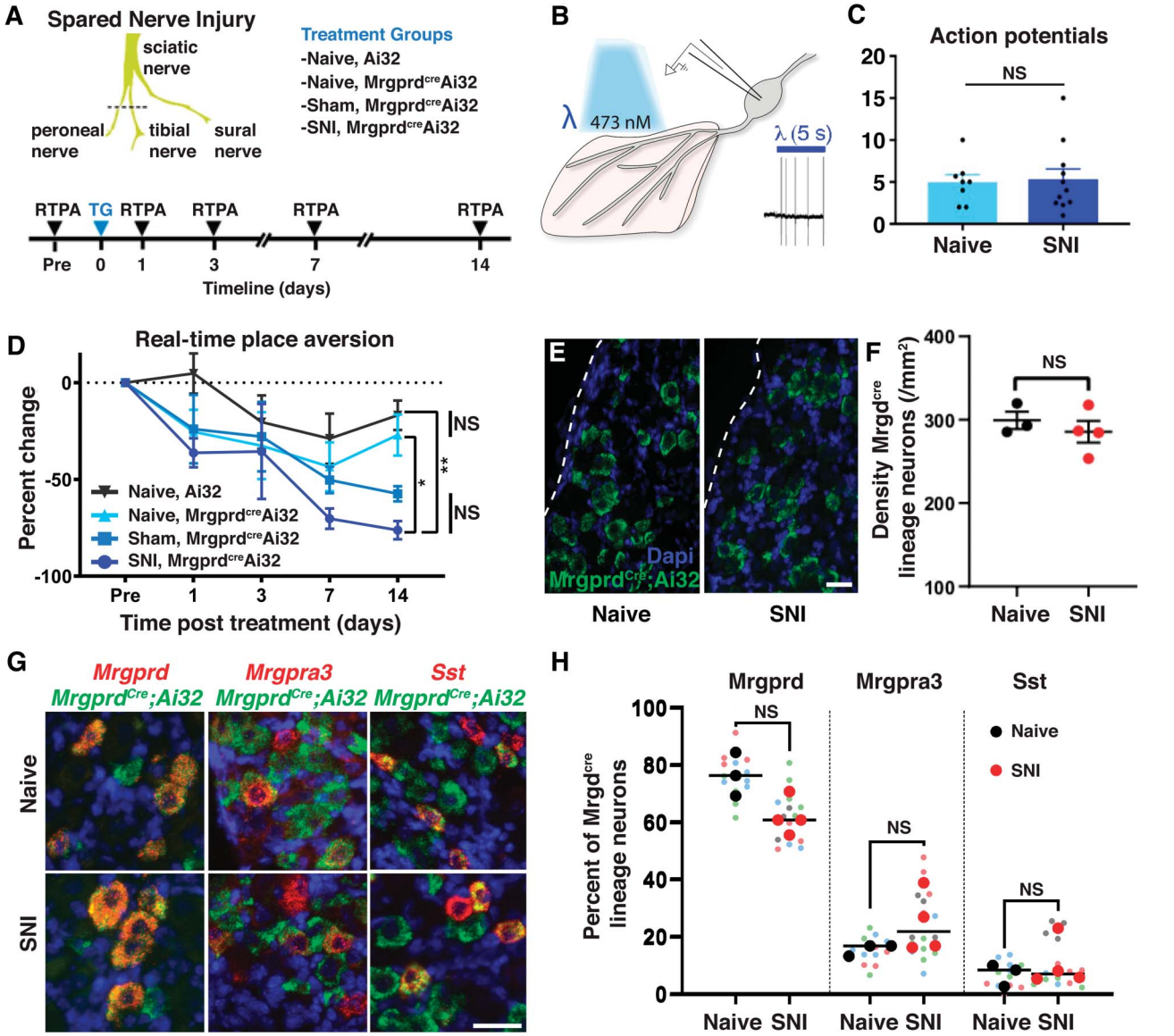

Figure 4. Optogenetic activation of *Mrgprd*^{Cre} lineage afferents is aversive after SNI. (A) Schematic illustrating experimental design. (B) Schematic and representative recording of responses of opto-tagged C fibers to cutaneous optogenetic stimulation in naive and SNI mice. (C) Quantification of the number of action potentials observed on optogenetic stimulation of the skin in individual neurons from naive and SNI *Mrgprd*^{Cre}; Ai32 mice. Data are mean ± SEM with dots representing data from individual neurons; N.S. indicates $P > 0.05$ (unpaired Student *t* test). (D) Real-time place aversion across 4 treatment groups: naive controls (no ChR2), naive *Mrgprd*^{Cre}; Ai32, sham *Mrgprd*^{Cre}; Ai32, and SNI *Mrgprd*^{Cre}; Ai32. Data are mean ± SEM. n = 5 to 6 mice per group. There was a significant main effect of time: $F(4, 76) = 14.82$, $P < 0.0001$; treatment groups: $F(3, 19) = 3.566$, $P = 0.0336$; and subject: $F(19, 76) = 2.433$, $P = 0.0034$ (2-way repeated measures ANOVA). N.S. indicates $P > 0.05$, $^{*}P < 0.05$, $^{**}P < 0.01$ (Tukey multiple comparisons test comparing main effect within treatment groups for each time point). All statistically significant post hoc comparisons are shown. There was no significant interaction between time and treatment. (E–F) Representative image and quantification of RNA FISH of L2 to L3 DRG from naive and SNI mice using probes against *Eyfp* to quantify ChR2-eYFP expressing cells. Scale bar = 50 μm. Data are mean ± SEM with individual animal averages shown as colored dots. N.S. indicates $P > 0.05$ (unpaired Student *t* test). (G–H) Representative images and quantification of the relative abundance of primary afferent populations within *Mrgprd*^{Cre} lineage cells in L2-L3 DRG from naive and SNI mice through multiplex FISH. Data are shown as a Superplot[18] that shows both the technical replicates (DRG sections, small-colored dots) and mean value for each animal (large dots). Each small-colored dot = 1 DRG section, and the color indicates from which animal the slice was taken (n= 3-4 mice per group). One-way ANOVA followed by post hoc comparisons were performed using Šídák multiple comparisons test comparing SNI with naive groups for each probe combination. N.S. indicates $P > 0.05$. ANOVA, analysis of variance; DRG, dorsal root ganglia; FISH, fluorescence in situ hybridization; SNI, spared nerve injury.

neurons using the ex vivo somatosensory preparation (**Fig. 5A**). Optogenetic stimulation of either the peripheral or central terminals gave rise to EPSCs onto recorded neurons in lamina I, albeit with different latencies (**Fig. 5B**). We also noted that the EPSC magnitude was larger when the optogenetic stimulation occurred at the skin rather than at the dorsal horn (**Fig. 5C**). However, there were several instances in which optogenetic stimulation at the dorsal horn was efficacious, whereas stimulation at the skin was not, likely reflecting the fact that not all recorded neurons had RFs in the skin of the dorsal hind paw. For this reason, we selected central stimulation for subsequent experiments.

We found that optogenetic activation of the central terminals of *Mrgprd*^{Cre} lineage neurons gave rise to EPSCs in only 6 of 27 random lamina I neurons (**Figs. 5D and E**). By contrast, optogenetic activation of the central terminals of *Trpv1*^{Cre} lineage neurons gave rise to EPSCs in 6 of 8 random lamina I neurons, which represented a significantly higher proportion relative to *Mrgprd*^{Cre} (Fisher exact test; $P < 0.05$). Moreover, optogenetic activation of afferents in

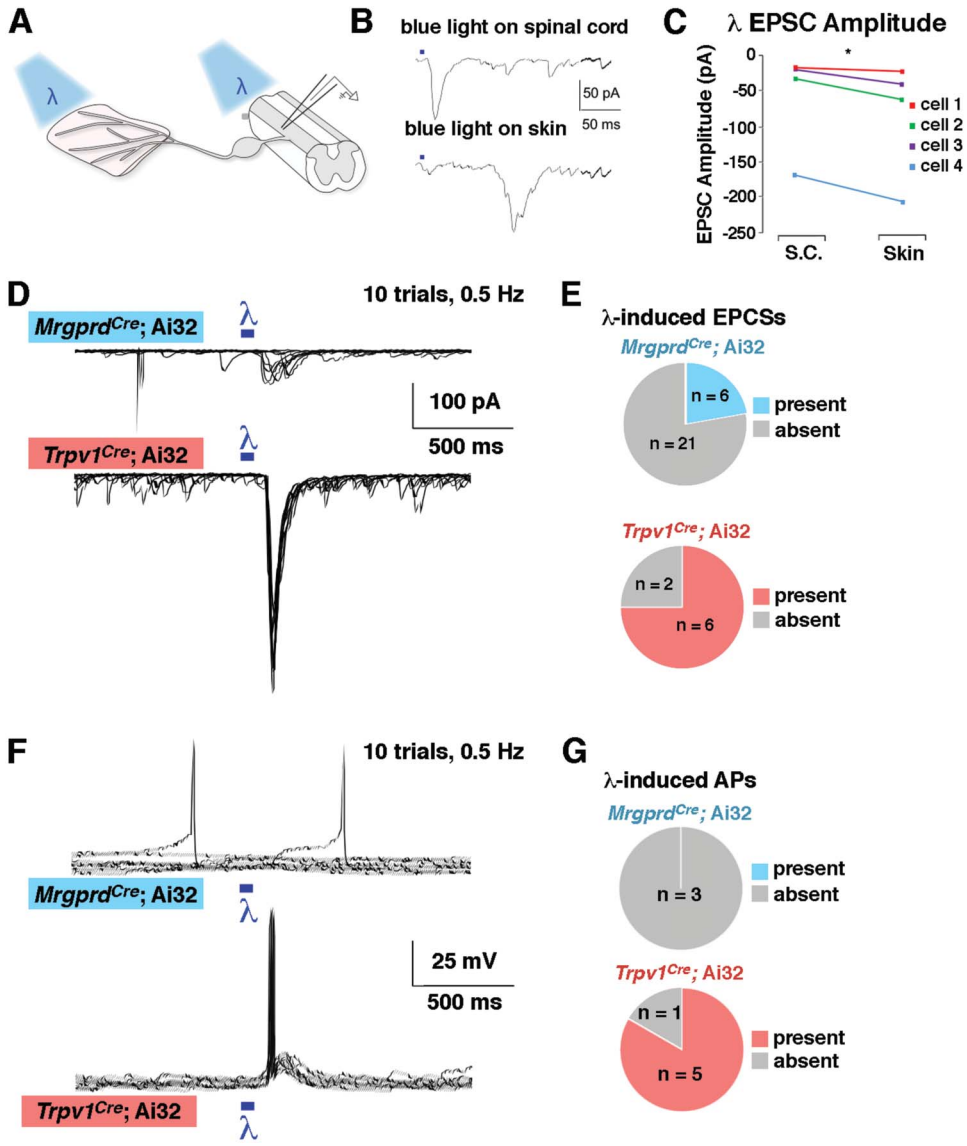

Figure 5. Lamina I neurons receive strong input from *Trpv1*^{Cre} lineage afferents but weak input from *Mrgprd*^{Cre} lineage afferents (A) Schematic of recordings with optogenetic stimulation at either the peripheral or central terminal. (B–C) Representative traces and quantification of EPSC amplitude from lamina I neurons after optogenetic stimulation at either the skin or the spinal cord. *$P < 0.05$ (paired Student *t* test). (D and E) Representative voltage clamp recordings ($V_H = -70$) and quantification of the proportion of lamina I neurons that show EPSCs on optogenetic stimulation at the spinal cord in *Mrgprd*^{Cre}; Ai32 and *Trpv1*^{Cre}; Ai32 mice. (F–G) Representative current clamp recordings and quantification of the proportion of lamina I neurons that show action potentials on optogenetic stimulation at the spinal cord in *Mrgprd*^{Cre}; Ai32 and *Trpv1*^{Cre}; Ai32 mice. For D and F, the responses to 10 stimulus presentations are superimposed. EPSC, excitatory postsynaptic currents.

Trpv1^{Cre}; Ai32 mice was sufficient to generate APs in 5 of 6 neurons that exhibited EPSCs, whereas the optogenetic activation in *Mrgprd*^{Cre}; Ai32 mice was insufficient to generate APs in lamina I cells (**Figs. 5F and G**), which again represented a significantly lower proportion than that observed on activation of *Trpv1*^{Cre} lineage neurons (Fisher exact test; $P < 0.05$). Because randomly targeted neurons are predominantly interneurons, these observations suggest that *Mrgprd*^{Cre} lineage neurons do not provide strong excitatory input, either directly or indirectly, onto lamina I interneurons.

3.6. Contribution of Mrgprd^{Cre} *lineage afferents to aversion after spared nerve injury*

Our behavioral experiments suggested that *Mrgprd*^{Cre} lineage input only became aversive after SNI. To investigate mechanisms that may contribute to this injury-induced change, we performed whole-cell recordings from lamina I SPB neurons in naive or SNI animals (**Fig. 6A**). In naive mice, less than half of lamina I SPB neurons displayed EPSCs in response to brushing of the skin with a paint brush, and this input led to APs in only 2 of the 12 cells (**Fig. 6B**). After nerve injury, however, 100% (13 of 13) lamina I SPB neurons showed EPSCs in response to the same dynamic, low-threshold input. Moreover, brushing of the skin from SNI mice resulted in APs in approximately 70% of LI SPB neurons in SNI mice, representing a 4-fold increase compared with that in naive mice. These results raise the possibility that allodynia in SNI mice may be caused by increased LI spinal output to low-threshold stimuli, such as brushing.

Next, we began investigating the contribution of *Mrgprd*^{Cre} lineage neurons to this abnormal spinal output. In naive mice, 7 of the 12 lamina I SPB neurons showed optogenetically induced EPCSs on stimulation of *Mrgprd*^{Cre} lineage afferents at 2 Hz. After SNI, however, this proportion increased

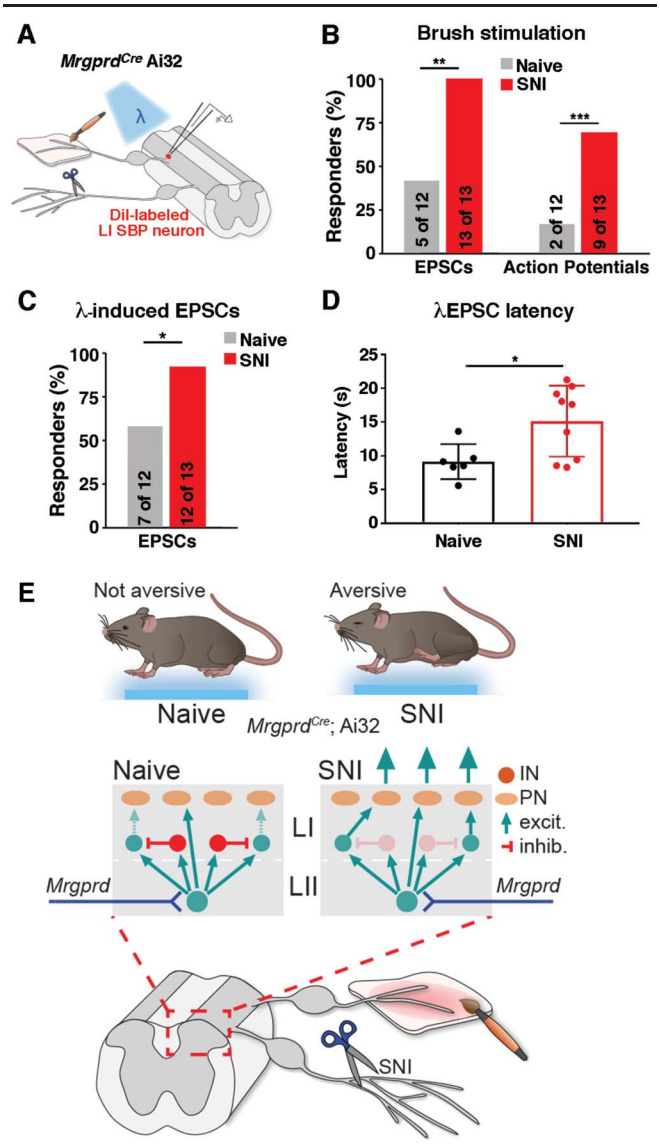

Figure 6. Increased proportion of lamina I SPB neurons are activated after brush and optogenetic stimulations of *Mrgprd*^{Cre} lineage afferents neurons after SNI. (A) Schematic showing patch clamp recordings of lamina I SPB neurons with brush or optogenetic stimulation. (B) Percentage of lamina I SPB neurons that show either EPSCs or action potentials (APs) in response to brushing of the skin in naive mice or those with SNI. $^{**}P < 0.01$ and $^{***}P < 0.001$ relative to naive (1-sided χ^2 test). (C) Percentage of lamina I SPB neurons that show EPSCs on optogenetic stimulation of *Mrgprd*^{Cre} lineage neurons in naive and SNI mice. $^{*}P < 0.05$ (1-sided χ^2 test). (D) EPSC latency to optogenetic stimulation of *Mrgprd*^{Cre} lineage neurons in naive mice or those with SNI. $^{*}P < 0.05$ relative to naive (unpaired, Student *t* test). (E) Proposed model of spinal circuitry activated by *Mrgprd*^{Cre} lineage neurons before and after SNI. SNI, spared nerve injury; EPSC, excitatory postsynaptic currents; SPB, spinoparabrachial.

significantly, with 12 of the 13 lamina I SPB neurons now responding to optogenetic stimulation (**Fig. 6C**). It should be noted, however, that this emergent *Mrgprd*^{Cre} lineage neuron input was still rarely sufficient, in itself, to elicit an action potential in the recorded output neuron. Thus, although *Mrgprd*^{Cre} lineage neurons are unlikely to be the only afferents involved in allodynia, they may, nevertheless, provide an important contribution. To gain insight into the underlying mechanism, we analyzed the EPCSs in more detail. Although a higher fraction of lamina I neurons showed light-induced EPSCs after SNI, the responses in individual neurons to optogenetic stimulation were similar, and we saw no evidence of synaptic sensitization. Instead, we found that the average response latency to optogenetic stimulation was significantly increased after SNI (**Fig. 6D**). This elevated latency implies that the enhanced number of responders to *Mrgprd*^{Cre} lineage stimulation occurs through an emergent polysynaptic pathway that is normally silent in naive mice (**Fig. 6E**).

4. Discussion

Our study provides evidence that activation of *Mrgprd*^{Cre} lineage afferents in a naive state is not aversive but becomes aversive in the context of chronic neuropathic pain caused by SNI. At the circuit level, we found that lamina I SPB neurons show significantly more brush-induced activity after nerve injury, which is an attractive mechanism to account for the phenomenon of mechanical allodynia. Moreover, *Mrgprd*^{Cre} lineage afferents may contribute to this abnormal spinal output after SNI because more lamina I SPB neurons receive *Mrgprd*^{Cre} lineage afferent input after optogenetic activation relative to naive controls. Finally, this increased input seems to be due to an emergent polysynaptic pathway, as evidenced by an increase in the average response latency to optogenetic stimulation of *Mrgprd*^{Cre} lineage afferents. Altogether, our study suggests that SNI gives rise to changes in spinal circuitry that enables increased brush-evoked activity in lamina I SPB neurons and that this effect is likely due, at least in part, to increased input from *Mrgprd*^{Cre} lineage afferents through a polysynaptic neural pathway that is normally silent in naive mice.

Previous studies have identified many mechanisms of injury-induced plasticity in the dorsal spinal cord.[2,30] Our data suggest that one of these mechanisms involves the engagement of a polysynaptic circuit that emerges after SNI, as evidenced by the increased average latency of input from nonpeptidergic afferents. These findings are consistent with the idea that allodynia after nerve injury is caused by disinhibition, which results in low-threshold stimuli abnormally reaching nociceptive pathways in the superficial dorsal horn.[27]

The results presented in this study show that low-frequency activation of cutaneous *Mrgprd*^{Cre} lineage afferents does not induce aversive behaviors. This lineage represents most C fibers innervating the skin. Thus, an important question is, what information is being conveyed during low-frequency activation of these fibers? One potential answer to this question is found in a recent study looking at parallel ascending SPB pathways projecting to distinct subsets of lateral parabrachial subnuclei.[7] They found that activation of one of these SPB pathways (GPR83, which is associated with cutaneous mechanosensation) could have either a positive or negative valence depending on the intensity of the optogenetic stimulation. Therefore, low-intensity activation of these fibers could possibly evoke a sensation of innocuous touch.

One of the limitations of this type of study is that optogenetic stimulation does not perfectly mimic natural stimulation. In this case, we found that light-mediated activation gave rise to APs in *Mrgprd*^{Cre} lineage afferents that was similar in frequency to that observed on stimulation with low-threshold stimuli (eg, 10 mN), but we did not achieve the instantaneous firing frequencies that are typically observed on stimulation with high-threshold stimuli (eg, 50 mN). For this reason, we cannot exclude the possibility that increasing the frequency of APs generated by optogenetic stimulation would alter its valence. Nevertheless, activation of this population at low frequency (2 Hz) is clearly not aversive in naive mice, whereas activation of afferents that include the cutaneous peptidergic C fibers is aversive. This important distinction raises the possibility that the bona fide nociceptors—those whose main function is to warn the

organism of tissue damage—are primarily represented by peptidergic C fibers and that the function of nonpeptidergic C fibers is likely to be much more nuanced and context dependent.

An unexpected finding of our work was that control mice lacking ChR2 expression, nevertheless, showed a modest degree of avoidance for the blue-light side of the RTPA apparatus that emerged after repeated exposure. Because both sides of the chamber produce equally low levels of thermal radiation, it is likely that this avoidance was in response to visual, rather than cutaneous, input. Moreover, mice avoided blue over amber light despite similar lux (illuminance), suggesting that it is the wavelength of light that contributes to the avoidance. We found that the avoidance observed in control mice was most pronounced when light was on continuously. By contrast, the optogenetically induced aversion in *Trpv1*^{Cre}; Ai32 mice was most pronounced when the light was on transiently, flashing at 2 Hz. Because optogenetic stimulation in the wind-up mode gave rise to the highest degree of aversion and, thus, seemed to be the most effective, we selected this stimulation paradigm for the behavioral experiments involving SNI. However, we note that it will be important to investigate a wide range of stimulation frequencies, including ones that we were not able to achieve with the current tools, to get a more complete picture of the relationship between stimulation frequency and perceptual percept.

Despite the caveat that mice are able to see cutaneous optogenetic stimulation through the floor in RTPA studies, we believe that this approach is still preferable to the implantation of fibers or LEDs through a surgical manipulation because the activation of cutaneous afferents with light does not involve tissue damage, which is likely to be confounding in pain studies. In this regard, it is noteworthy that sham-operated mice that expressed ChR2 in *Mrgprd*^{Cre} lineage afferents also showed a trend toward avoidance of the blue side of the RTPA chamber that was greater than that observed in naive mice, although not as pronounced as that observed in SNI mice. This intermediate phenotype of sham treatment suggests that the surgical procedure involving the cutting of skin and muscle is in itself an injury model that may be sufficient for ongoing changes in spinal circuitry.

Just as previously reported,[17] we found that Mrgpra3-expressing afferents and Sst-expressing afferents are derived from the Mrgprd lineage. Intriguingly, all 3 of these afferent subtypes show predominant (although not exclusive) cutaneous targeting, and all 3 have been implicated in itch.[11,13,16,21,26] We did not observe itch behaviors—scratching or biting —on optogenetic activation of *Mrgprd*^{Cre} lineage afferents in our study. Curiously, itch behavior seems to be more dramatic on chemogenetic (rather than optogenetic) activation of these populations.[11,21,24] We speculate that it is not simply the type of afferent input but also the pattern and the frequency of activation that are interpreted by the nervous system to differentially represent itch, pain, and some aspects of touch. Understanding this integration is of fundamental importance to our basic understanding of somatosensation and may one day lead to the development of improved strategies for the treatment of pain.

Conflict of interest statement

The authors have no conflicts of interest to declare.

Acknowledgments

The research reported in this publication was supported by the National Institute of Neurological Disorder and Stroke of the National Institutes of Health under Award Number R01 NS096705 to H.R. Koerber, NS073548 to C. Warwick, NS110155 to T.D. Sheahan, and the National Institute of Arthritis and Musculoskeletal and Skin Diseases of the National Institutes of Health under Award Number R01AR063772 to S.E. Ross.

Supplemental video content

A video abstract associated with this article can be found at http://links.lww.com/PAIN/B301.

Article history:
Received 23 September 2020
Received in revised form 7 January 2021
Accepted 13 January 2021
Available online 4 February 2021

References

[1] Adelman PC, Baumbauer KM, Friedman R, Shah M, Wright M, Young E, Jankowski MP, Albers KM, Koerber HR. Single-cell q-PCR derived expression profiles of identified sensory neurons. Mol Pain 2019;15:1744806919884496.
[2] Basbaum AI. Spinal mechanisms of acute and persistent pain. Reg Anesth Pain Med 1999;24:59–67.
[3] Basbaum AI, Bautista DM, Scherrer G, Julius D. Cellular and molecular mechanisms of pain. Cell 2009;139:267–84.
[4] Beaudry H, Daou I, Ase AR, Ribeiro-da-Silva A, Seguela P. Distinct behavioral responses evoked by selective optogenetic stimulation of the major TRPV1+ and MrgD+ subsets of C-fibers. PAIN 2017;158:2329–39.
[5] Cavanaugh DJ, Chesler AT, Jackson AC, Sigal YM, Yamanaka H, Grant R, O'Donnell D, Nicoll RA, Shah NM, Julius D, Basbaum AI. Trpv1 reporter mice reveal highly restricted brain distribution and functional expression in arteriolar smooth muscle cells. J Neurosci 2011;31:5067–77.
[6] Cavanaugh DJ, Lee H, Lo L, Shields SD, Zylka MJ, Basbaum AI, Anderson DJ. Distinct subsets of unmyelinated primary sensory fibers mediate behavioral responses to noxious thermal and mechanical stimuli. Proc Natl Acad Sci U S A 2009;106:9075–80.
[7] Choi S, Hachisuka J, Brett MA, Magee A, Omori Y, Iqbal N, Zhang DH, Delisle MM, Wolfson RL, Bai L, Santiago C, Gong S, Goulding M, Heintz N, Koerber HR, Ross SE, Ginty DD. Parallel ascending spinal pathways for affective touch and pain. Nature 2020;587:258–63.
[8] Decosterd I, Woolf CJ. Spared nerve injury: an animal model of persistent peripheral neuropathic pain. PAIN 2000;87:149–58.
[9] Gatto G, Smith KM, Ross SE, Goulding M. Neuronal diversity in the somatosensory system: bridging the gap between cell type and function. Curr Opin Neurobiol 2019;56:167–74.
[10] Hachisuka J, Baumbauer KM, Omori Y, Snyder LM, Koerber HR, Ross SE. Semi-intact ex vivo approach to investigate spinal somatosensory circuits. Elife 2016;5:e22866.
[11] Han L, Ma C, Liu Q, Weng HJ, Cui Y, Tang Z, Kim Y, Nie H, Qu L, Patel KN, Li Z, McNeil B, He S, Guan Y, Xiao B, Lamotte RH, Dong X. A subpopulation of nociceptors specifically linked to itch. Nat Neurosci 2013;16:174–82.
[12] Handwerker HO, Forster C, Kirchhoff C. Discharge patterns of human C-fibers induced by itching and burning stimuli. J Neurophysiol 1991;66:307–15.
[13] Huang J, Polgar E, Solinski HJ, Mishra SK, Tseng PY, Iwagaki N, Boyle KA, Dickie AC, Kriegbaum MC, Wildner H, Zeilhofer HU, Watanabe M, Riddell JS, Todd AJ, Hoon MA. Circuit dissection of the role of somatostatin in itch and pain. Nat Neurosci 2018;21:707–16.
[14] Jensen TS, Finnerup NB. Allodynia and hyperalgesia in neuropathic pain: clinical manifestations and mechanisms. Lancet Neurol 2014;13:924–35.
[15] Lawson JJ, McIlwrath SL, Woodbury CJ, Davis BM, Koerber HR. TRPV1 unlike TRPV2 is restricted to a subset of mechanically insensitive cutaneous nociceptors responding to heat. J Pain 2008;9:298–308.
[16] Liu Q, Sikand P, Ma C, Tang Z, Han L, Li Z, Sun S, LaMotte RH, Dong X. Mechanisms of itch evoked by beta-alanine. J Neurosci 2012;32:14532–7.
[17] Liu Y, Yang FC, Okuda T, Dong X, Zylka MJ, Chen CL, Anderson DJ, Kuner R, Ma Q. Mechanisms of compartmentalized expression of Mrg

class G-protein-coupled sensory receptors. J Neurosci 2008;28: 125–32.
[18] Lord SJ, Velle KB, Mullins RD, Fritz-Laylin LK. SuperPlots: communicating reproducibility and variability in cell biology. J Cel Biol 2020;219:e202001064.
[19] Madisen L, Mao T, Koch H, Zhuo JM, Berenyi A, Fujisawa S, Hsu YW, Garcia AJ III, Gu X, Zanella S, Kidney J, Gu H, Mao Y, Hooks BM, Boyden ES, Buzsaki G, Ramirez JM, Jones AR, Svoboda K, Han X, Turner EE, Zeng H. A toolbox of Cre-dependent optogenetic transgenic mice for light-induced activation and silencing. Nat Neurosci 2012;15: 793–802.
[20] McIlwrath SL, Lawson JJ, Anderson CE, Albers KM, Koerber HR. Overexpression of neurotrophin-3 enhances the mechanical response properties of slowly adapting type 1 afferents and myelinated nociceptors. Eur J Neurosci 2007;26:1801–12.
[21] Mishra SK, Hoon MA. The cells and circuitry for itch responses in mice. Science 2013;340:968–71.
[22] Nguyen MQ, Wu Y, Bonilla LS, von Buchholtz LJ, Ryba NJP. Diversity amongst trigeminal neurons revealed by high throughput single cell sequencing. PLoS One 2017;12:e0185543.
[23] Rau KK, McIlwrath SL, Wang H, Lawson JJ, Jankowski MP, Zylka MJ, Anderson DJ, Koerber HR. Mrgprd enhances excitability in specific populations of cutaneous murine polymodal nociceptors. J Neurosci 2009;29:8612–19.
[24] Sharif B, Ase AR, Ribeiro-da-Silva A, Seguela P. Differential coding of itch and pain by a subpopulation of primary afferent neurons. Neuron 2020; 106:940–51 e944.
[25] Sharma N, Flaherty K, Lezgiyeva K, Wagner DE, Klein AM, Ginty DD. The emergence of transcriptional identity in somatosensory neurons. Nature 2020;577:392–8.
[26] Solinski HJ, Kriegbaum MC, Tseng PY, Earnest TW, Gu X, Barik A, Chesler AT, Hoon MA. Nppb neurons are sensors of mast cell-induced itch. Cell Rep 2019;26:3561–73 e3564.
[27] Torsney C, MacDermott AB. Disinhibition opens the gate to pathological pain signaling in superficial neurokinin 1 receptor-expressing neurons in rat spinal cord. J Neurosci 2006;26:1833–43.
[28] Usoskin D, Furlan A, Islam S, Abdo H, Lonnerberg P, Lou D, Hjerling-Leffler J, Haeggstrom J, Kharchenko O, Kharchenko PV, Linnarsson S, Ernfors P. Unbiased classification of sensory neuron types by large-scale single-cell RNA sequencing. Nat Neurosci 2015;18:145–53.
[29] Van Hees J, Gybels J. C nociceptor activity in human nerve during painful and non painful skin stimulation. J Neurol Neurosurg Psychiatry 1981;44:600–7.
[30] Woolf CJ. Central sensitization: implications for the diagnosis and treatment of pain. PAIN 2011;152(3 suppl):S2–15.